Landscape evolution in Val Mulix, eastern Swiss Alps – soil chemical and mineralogical analyses as age proxies

Böhlert, R ; Mirabella, A ; Plötze, M ; Egli, M

Abstract: Towards the end of the last glacial cycle, repeated re-advances of valley glaciers in the European Alps combined with periglacial processes led to the formation of a variety of climate-related landforms. Independent age measurements of moraines and rock glacier lobes using both in-situ produced and meteoric 10Be allows for the use of soil formation as an age proxy. In this complementary study we present chemical and mineralogical data from five Podzols from Val Mulix in Eastern Switzerland. Two of them developed on granitic Lateglacial moraines (14.9 ka and 10.7 ka, respectively) and three were sampled on lobes of a morphostratigraphically connected relict rock glacier, covering an age range of approx. 10.7 ka to 8.6 ka. Besides the evaluation of the suitability of selected pedosignatures for a relative age separation, we hypothesised that these pedosignatures should give further information about the evolution of the specific sites. Although the soils had a high skeleton content and the oldest soil started its development in a slightly colder climatic phase, typical weathering trends could still be detected. Whereas weathering indices such as the (K + Ca)/Ti ratio or the B-index reflect time trends reasonably well, the mineralogical composition of the fine earth and clay fraction yielded a slightly more inconsistent picture; to a lesser extent, some inconsistencies were also exhibited when using the weathering mass balance approach. This is especially true for the relict rock glacier and it supports the suggested complex development history of these soils as well as the presence of pre-weathered material. Techniques that include several surface soil horizons and the soil skeleton such as the (K + Ca)/Ti ratio, the B-index and the mass balance approach gave more robust results (in terms of the expected chronology) than the ones that only referred to single horizons (clay mineralogy). Errors or variations due to potential reallocation processes within the soil horizons but without a prominent change of the overall soil characteristics are minimised using such an approach. Weathering indexes and the clay mineral assemblage provided a differentiation of soils even within a relatively narrow time range and gave insight into processes that have occurred at the specific sites. The combined relative-numerical dating approach used here not only enables an extended interpretation and mutual control, but ultimately leads to a better understanding of landscape reconstruction and evolution.

DOI: https://doi.org/10.1016/j.catena.2011.06.013

DOI: https://doi.org/10.1016/j.catena.2011.06.013

Landscape evolution in Val Mulix, eastern Swiss Alps – Soil chemical and mineralogical analyses as age proxies

Ralph Böhlert[1], Aldo Mirabella[2], Michael Plötze[3], Markus Egli[1]*

[1]Department of Geography, University of Zurich, CH-8057 Zurich, Switzerland

[2]Centro di ricerca per l'agrobiologia e la Pedologia (CRA-ABP), Florence, Italy

[3]Institute for Geotechnical Engineering, ETH Zurich, CH-8093 Zurich, Switzerland

*E-mail of the corresponding author: markus.egli@geo.uzh.ch

Abstract

Towards the end of the last glacial cycle, repeated re-advances of valley glaciers in the European Alps combined with periglacial processes led to the formation of a variety of climate-related landforms. Independent age measurements of moraines and rock glacier lobes using both in-situ produced and meteoric ^{10}Be allows for the use of soil formation as an age proxy. In this complementary study we present chemical and mineralogical data from five Podzols from Val Mulix in Eastern Switzerland. Two of them developed on granitic Lateglacial moraines (14.9 ka and 10.7 ka, respectively) and three were sampled on lobes of a morphostratigraphically connected relict rock glacier, covering an age range of approx. 10.7 ka to 8.6 ka. Besides the evaluation of the suitability of selected pedosignatures for a relative age separation, we hypothesised that these pedosignatures should give further information about the evolution of the specific sites. Although the soils had a high skeleton content and the oldest soil started its development in a slightly colder climatic phase, typical weathering trends could still be detected. Whereas weathering indices such as the (K+Ca)/Ti ratio or the B-index reflect time trends reasonably well, the mineralogical composition of the fine

earth and clay fraction yielded a slightly more inconsistent picture; to a lesser extent, some inconsistencies were also exhibited when using the weathering mass balance approach. This is especially true for the relict rock glacier and it supports the suggested complex development history of these soils as well as the presence of pre-weathered material. Techniques that include several surface soil horizons and the soil skeleton such as the (K+Ca)/Ti ratio, the B-index and the mass balance approach gave more robust results (in terms of the expected chronology) than the ones that only referred to single horizons (clay mineralogy). Errors or variations due to potential reallocation processes within the soil horizons but without a prominent change of the overall soil characteristics are minimised using such an approach. Weathering indexes and the clay mineral assemblage provided a differentiation of soils even within a relatively narrow time range and gave insight into processes that have occurred at the specific sites. The combined relative-numerical dating approach used here not only enables an extended interpretation and mutual control, but ultimately leads to a better understanding of landscape reconstruction and evolution.

Keywords: Alpine landscape evolution, soils, weathering, dating

1. Introduction

The time span between the melt back of the glaciers after the Last Glacial Maximum (LGM, around 21 ka: Ivy-Ochs et al., 2004) and the transition to the Holocene approx. 11.5 ka ago, was subjected to a very unstable and fast changing climate. In this period which is referred to as the 'Alpine Lateglacial' (Penck and Brückner, 1909) and the following early Holocene, repeated glacier re-advances combined with periglacial processes resulted in a variety of still-visible landforms such as moraines or rock glaciers. Dating of such climate related landforms allows the estimation of process rates and gives an impression of the sensitivity of high Alpine regions to rapidly changing climatic conditions. Using mapping techniques based on relative moraine positions, moraine morphology and cal-

culation of equilibrium line altitude (ELA) depression values (Accumulation Area Ratio AAR = 0.67 with LIA (Little Ice Age) moraines as reference; AAR is the ratio of the accumulation area to the total area of the glacier), an assignment of morainic sequences to different 'stadials' was established (e.g. Gross et al., 1977; Maisch, 1981; Keller and Krayss, 1993). With the discovery of the radiocarbon method and progress in the usage of cosmogenic isotopes produced in situ in rock surfaces (Lal, 1988; Gosse and Phillips, 2001), it became possible to date more reliably the deposition of moraines, the formation of peat bogs and sediments, the occurrence of landslides and other geomorphic phenomena. This absolute chronology of glacier (re)advance and retreat phases, however, is definitely not complete and additional data is needed.

Radiometric dating methods are comparatively expensive and sample preparation is laborious. Additionally, organic material for radiocarbon dating may be lacking, or only a restricted number of moraine boulders suitable for surface-exposure dating is available. In such cases when the database is rather weak, the combined application of additional relative methods is meaningful and can give precious indications about possible error sources and reduces uncertainties in the interpretation of numerical ages. Soils are traditionally understood as a function of the state-factors parent material, climate, topography, biological activity and time (Jenny, 1941). Consequently, by choosing sampling sites minimising the effect of soil forming factors other than time, the influence of time on soil formation can be studied (chronosequence). Soils sampled on moraines and other glacial and periglacial deposits such as rock glaciers can either be helpful indicators to estimate the (relative) age of the landform or, provided that independent dating is available, to derive rates of different time-dependent processes (Egli et al., 2001, 2003; Munroe, 2008; Schaller et al., 2009). Soil characteristics commonly show variations across the landscape. Therefore, when used as an age indicator, soil development data should be combined with other relative or numerical age data (Dahms, 2004). Chemical and mineralogical analyses of soil chronosequences offer several methods of distinguishing landforms of different ages based on their weathering state (Alexander and Burt, 1996; Evans,

1999; Egli et al., 2001, 2003). Well-known soil age indicators are for instance soil pH, rubification, transformation of pedogenic Fe and Al (Birkeland, 1999) and the presence of clay minerals such as smectite (Righi et al., 1999). However, most of them are not applicable to old soils in alpine areas as the greatest changes in soil properties occur within approximately 3000 – 4000 years, reaching a kind of asymptotic value after about 15 ky (cf. Egli et al., 2001; Fitze, 1982).

In this complementary study we present soil chemical and mineralogical aspects of five soil profiles developed on two Lateglacial moraines and three lobes of a morphologically associated relict rock glacier (Fig. 1 and Fig. 2). Age control is given by surface exposure ages using cosmogenic ^{10}Be produced in situ (Böhlert et al., 2011). Additionally, in case of profile S1 (see Fig. 1 and 2 and Table 1 for the position and description of the sampling sites), the age calculation based on the inventory of meteoric ^{10}Be (Egli et al., 2010) is available. Besides the measurement of standard soil chemical and physical properties, the methods applied here include the calculation of soil element losses as well as mineralogical analyses (qualitative and quantitative). A main aim was whether a relative age separation of surfaces was possible using selected pedosignatures. We, furthermore, hypothesised that these pedosignatures should give additional indications about the evolution of the specific sites.

2. Study area and sampling sites

Val Mulix is located in the eastern part of the Swiss Alps. An overview is given in Figure 1. The region is situated in the Err-Bernina nappe that belongs to the lower Austroalpine. The greenish 'Albula Granite' is the dominating rock type (Bearth et al., 1987), constituting the parent material of all five sampling sites (Table 2). The Albula-Granite provides the source material for all samples taken in this area. Mesozoic sedimentary rocks are very sparse (Bearth et al.,1987) and their influence to parent material chemistry is negligible. The mean annual precipitation in the investigation area increases with altitude from approximately 1000 to 1300 mm (EDI, 1992). As all sampling

sites are in the same catchment area and at approximately the same altitude (Table 1), no significant differences in precipitation are to be expected. The sampling site S1 is the only one in a forest. *Larix decidua* and *Pinus cembra* are the main constituents, accompanied by *Rhododendron ferrugineum*. At the other sampling sites, dwarf-shrubs, mostly Ericaceae, single trees (*Larix decidua, Pinus cembra*), and alpine grassland are characteristic (Table 1).

In Val Mulix, numerous glacial and periglacial landforms from the Lateglacial and the early Holocene time periods can be found (Fig. 1). Based on geomorphologic mapping (Maisch, 1981), the moraines in this valley generally belong to the 'Daun' and the 'Egesen stadial'. These are locality types describing a relative assignment of moraine sequences formed as a result of Lateglacial glacier re-advances on a supra-regional scale in the European Alps (Heuberger, 1966). Based on numerical datings (for an overview see Ivy-Ochs et al., 2008) it is widely accepted that the often threefold Egesen moraines (Egesen I – III) were deposited in the Younger Dryas. In contrast, numerical ages for Daun moraines are broadly lacking.

Profile S1 was taken on a confluence moraine of the former Mulix and Tschitta glacier (Figs. 1 and 2). This moraine was mapped as a Daun moraine (Maisch, 1981) that could be supported by a ^{10}Be age of 14.9 ± 1.8 ka (Böhlert et al., 2011). This means it was most probably deposited before the Bølling /Allerød interstadial (Oldest Dryas). A very similar age of 14.3 ± 2.3 ka was determined using the inventory of meteoric ^{10}Be of this soil profile (Egli et al., 2010). Profile S3 was taken on the orographically right lateral Egesen moraine that yielded a ^{10}Be age of 10.7 ± 0.9 ka (Böhlert et al., 2011). Another Egesen moraine is just some 20 m above. Even more upslope, a Daun moraine can be found that is strongly influenced by creeping processes and only remnants are left. Although these two moraines were not sampled for soil analysis, they probably played an important role for the rock glacier formation by providing source material during the initiation of rock glacier activity (see below). Profiles S2, S4 and S5 were taken on rock glacier lobes in the tongue area, in the middle part and in the upper part near the root zone, respectively. The discordant geomorphologic situa-

126 tion shows that rock glacier and moraine geneses are interconnected. After retreat of the main ice
127 body, a debris mass, which was obviously dammed behind the lateral moraine, began to move
128 downslope under permafrost conditions, thereby creating a breach into the Egesen moraine (Fig. 1).
129 This setting makes clear that this (nowadays) relict rock glacier must be younger than the Egesen
130 advance. At least at an initial stage, the source material could have been provided mainly by an
131 above-deposited and deformed Daun moraine and the Egesen moraines themselves. Later on, an
132 additional debris supply from the headwall must be assumed; otherwise the formation of an almost
133 700 m-long rock glacier does not seem possible. As a result, the rock glacier contains more fine-
134 grained (morainic) material than usual. This created the precondition for a comparable well-
135 pronounced soil development with clearly identifiable horizons, especially in the lower and the
136 middle part of the rock glacier.
137 Surface exposure dating (^{10}Be) on big boulders in the tongue area and in the root zone of the rock
138 glacier yielded 12.6 ± 0.9 ka and 8.6 ± 0.6 ka, respectively. Whereas the date from the root zone can
139 be accepted as an indication for the timing of inactivation in the early Holocene, the age from the
140 tongue seems too old to correspond to the age of the sampled Egesen moraine (10.7 ± 0.9 ka) that
141 was cut across. A meaningful explanation for this apparently contradictory situation is an initial
142 deposition of this boulder on the Egesen moraine upslope from the sampled one (Fig. 1 and 2). This
143 means that this age from near S2 (12.6 ± 0.9 ka) represents in fact the timing of the most extensive
144 Egesen advance that is in full agreement with ages found in literature (Ivy-Ochs, 2008). The age of
145 the sampled Egesen moraine (10.7 ± 0.9 ka) can be understood as a minimum age for the beginning
146 of the activity phase. This agrees well with the hypothesis of Maisch (1981), suggesting a main ac-
147 tivity phase of the rock glacier contemporaneous to the Egesen II advance, i.e. towards the end of
148 the Younger Dryas. Based on the morphostratigraphic situation and numerical ^{10}Be-ages available,
149 the following order of soil ages has to be expected: Daun moraine (S1) > Egesen moraine (S3) ≥
150 Rock glacier lower part (S2) > rock glacier middle part (S4) > rock glacier upper part (S5).

151

152 **3. Materials and methods**

153

154 *3.1. Sampling strategy and soil chemistry/physics*

155 Soil material was collected from excavated profile pits on undisturbed locations where no influence
156 of creeping processes was visible. If possible, profiles were dug down to the C horizon. 2-3 kg of
157 soil material per horizon were taken for the analyses (Hitz et al., 2002). Colours were determined
158 based on the Munsell colour system and the bulk density (fine earth and soil skeleton) measured
159 using a specific soil core sampler.

160 The oven-dried (60°C) samples were sieved to < 2 mm and ball-milled for determination of C and
161 N contents with a C/H/N-analyser (Elementar Vario EL, elementar Analysensysteme GmbH). Soil
162 pH was measured in 0.01 M $CaCl_2$ using a soil solution ratio of 1:2.5. A combination of wet sieving
163 for particles 2000 – 32 µm and X-ray sedimentometry (SediGraph 5100) for finer particles < 32 µm
164 was applied for analyzing the particle size distribution.

165 Fe, Al and Si concentrations were determined after treatment with sodium-dithionite (labelled with
166 'd', e.g. Fe_d) and NH_4-oxalate (buffered at pH 3, label 'o'), respectively (McKeague et al., 1971).
167 The extracts were centrifuged for 8 minutes at 4000 rpm and filtered (mesh size 0.45 µm, S&S, fil-
168 ter type 030/20). Element concentrations were measured using atomic absorption spectroscopy
169 (AAnalyst 700, Perkin Elmer). The amount of well crystalline Fe-oxide was calculated by the dif-
170 ference between its dithionite and oxalate extractable content ($Fe_d - Fe_o$). With respect to the Al/Si
171 molar ratio, the sum of imogolite and proto-imogolite allophane ('Imogolite-type material', ITM)
172 was calculated as follows (Parfitt et al., 1988):

173 $$\mathrm{ITM} = f \cdot \mathrm{Si_o}(\%) \qquad (1)$$

174 with

175 $$f = 5 + 2.1 \cdot \left(\frac{Alo}{Sio} - 1 \right) \qquad (2)$$

176 with Al_o and Si_o as the oxalate-extractable Al and Si (both in moles), respectively. In this calcula-
177 tion, the sodium-pyrophosphate Al-fraction (Al_p) was not considered (although some horizons may
178 have some Al_p that should be subtracted from Al_o to obtain the ITM content). Consequently, equa-
179 tion 1 only gives a rough estimation. According to Parfitt and Childs (1988) the concentration of
180 ferrihydrite can be performed using $1.7 \cdot Fe_o$.
181 Measurement of the total element content of fine earth and skeleton was done by means of X-ray
182 fluorescence (XRF). Around 10 g of soil material were milled to < 50 µm in a tungsten carbide disc
183 swing mill (Retsch® RS1, Germany). 4 g of soil powder was mixed with 0.9 g of Licowax® C Mi-
184 cro-Powder PM (Clariant, Switzerland), pressed into a 32 mm-pellet and analysed using an energy
185 dispersive X-ray fluorescence spectrometer (SPECTRO X-LAB 2000, SPECTRO Analytical In-
186 struments, Germany).
187
188 *3.2. Calculation of mass balance based on immobile elements*
189 Differences in chemical composition of fresh source rock and soil material can be used to derive
190 weathering properties. In most cases, chemical and biophysical weathering is not isovolumetric and
191 an elementary volume may dilate or collapse during soil evolution. Considering these enrich-
192 ment/depletion factors determined using concentration profiles of immobile elements such as Ti or
193 Zr, element specific gains and losses and, in case of known landform ages, long-term weathering
194 rates can be calculated; for theoretical and mathematical background, see Chadwick et al. (1990)
195 and Egli and Fitze (2000)). Volumetric changes that occur during pedogenesis were determined by
196 adopting the classical definition of strain, $\varepsilon_{i,W}$ (Brimhall and Dietrich, 1987):

197 $$\varepsilon_{i,w} = \frac{\Delta z_w}{\Delta z} - 1 \qquad (3)$$

198 with Δz as the columnar height (m) of a representative elementary volume of protore (or unweath-
199 ered parent material) p and Δz_W is the weathered equivalent height (m) w. The calculation of the
200 open-system mass transport function $\tau_{j,W}$ is defined by (Chadwick et al., 1990):

201 $$\tau_{j,w} = \left(\frac{\rho_w C_{j,w}}{\rho_p C_{j,p}} \left(\varepsilon_{i,w} + 1 \right) \right) - 1 \qquad (4)$$

202 where $C_{j,p}$ (kg/t) is the concentration of element j in protolith (e.g., unweathered parent material,
203 bedrock), $C_{j,W}$ is the concentration of element j in the weathered product (kg/t), and with ρ_p and
204 ρ_W represent the bulk density (t/m^3) of the protolith and the weathered soil, respectively. With n
205 soil layers, the calculation of changes in mass of element j is given by (Egli and Fitze, 2000)

206 $$\bar{m}_{j,flux(z_w)} = \sum_{a=1}^{n} C_{j,p} \rho_p \left(\frac{1}{\varepsilon_{i,w} + 1} \right) \tau_{j,w} \Delta z_w \qquad (5)$$

207 where $\tau_{j,W}$ corresponds to the mass transport function $\varepsilon_{i,W}$ to the strain, and Δz to the weathered
208 equivalent of the columnar height (m) of a representative elementary volume. As weathering not
209 only occurs in the fine earth fraction (e.g. Corti et al., 1998; Rossi and Graham, 2010), the soil
210 skeleton was also taken into account.
211 For soils developed in situ on bedrock the potential errors are confined to local heterogeneities in
212 bedrock composition. The estimate of the initial composition becomes more difficult when soils are
213 developed on sedimentary parent materials such as alluvial terraces, loess deposits, debris or morai-
214 nic material. For such deposits, the least weathered horizon in the soil profile is assumed to be the
215 parent material.
216 Several indexes have been defined to characterise chemical weathering in soils. The general princi-
217 ple of all these indexes is similar and based on the ratio of the base cations (Ca, Mg, K, Na) to Al
218 and/or Si. We used the index B according to Kronberg and Nesbitt (1981) that is defined by the mo-
219 lar ratio:

220 $$B = \frac{CaO + K_2O + Na_2O}{Al_2O_3 + CaO + K_2O + Na_2O} \quad (6)$$

221

222 *3.3. Separation of clay fraction and soil mineralogy*

223 To separate the clay fraction (< 2µm), the fine earth samples (< 2 mm) were pre-treated at room
224 temperature with diluted and Na-acetate buffered (pH 5) H_2O_2 (3%). The clay fraction was obtained
225 by dispersion with Calgon and sedimentation in water. Specimens were then Mg-saturated, washed
226 free of chloride and freeze-dried. Clay-aggregate samples, orientated on glass slides from a water
227 suspension, were analysed using a θ-2θ Philips PW1820 diffractometer (automatic theta compensat-
228 ing divergence slit, graphite monochromator) using Cu-Kα radiation (40 kV, 30 mA). Slides were
229 step-scanned from 2 to 15°2θ with steps of 0.02°2θ at 2 second intervals. The following treatments
230 were performed: Mg-saturation, ethylene glycol solvation and K saturation, followed by heating for
231 2 hours at 335 °C and 550 °C. When chlorite was present, the presence of kaolinite was checked
232 with FT-IR (Bruker Optics, Tensor 27) analysis (OH-stretching region near 3695 cm^{-1}) on powder
233 samples (3% milled soil material, 97% KBr) heated at 80 °C for ≥ 2 h. Digitised X-ray data were
234 smoothed and corrected for Lorentz and polarisation factors (Moore and Reynolds, 1997). Back-
235 ground values were calculated by means of a non-linear function (polynomial 2^{nd} order function;
236 Lanson, 1997). The *d*(060) region was studied on randomly oriented samples step-scanned from 58
237 to 64°2θ with steps of 0.02°2θ at 10 second intervals.
238 The semi-quantitative estimation of phyllosilicate concentration was performed by the combination
239 of the areas of the ethylene glycol solvated, Mg-saturated, the K-saturated and heated (335 °C and
240 550 °C) samples. On the basis of these integrals, an estimate of clay minerals composition was per-
241 formed. The sum of the areas between 2 and 15° 2θ, which were attributed to HIV (hydroxy inter-
242 layered vermiculites), smectite, vermiculite, mica, chlorite and kaolinite, were standardised to
243 100%. Although the (semi-)quantification of clay minerals in soils is bedevilled by manifold prob-
244 lems (Kahle et al., 2002), the applied and standardised (sample preparation, treatments, measure-

ment and calculation) procedure enabled the assessment of the variability of clay mineral assemblage amongst the sites.

The quantitative mineralogical composition of the inorganic part of the fine earth (fraction < 2 mm) was obtained using Rietveld analysis (program AutoQuan/BGMN, GE SEIFERT; Plötze et al., 2003; Omotoso et al., 2006) of XRD patterns of randomly oriented specimens (Bruker AXS D8 Advance, Cu-Kα, 4-70°2θ, 40kV, 40mA, 0.02°-steps, 4s/step, automatic theta compensating divergence and antiscattering slits, graphite monochromator).

4. Results

4.1. Chemical and physical characteristics of the soils

Except for S5, which was characterised by horizons that were more difficult to differentiate and by weathering pockets, the soils showed an undisturbed evolution with no signs of erosion or burial. According to the visual impression in the field, the soils on the moraines clearly showed a higher degree of development with more pronounced eluvial horizons (Fig. 2). All soils in the study area have a sandy loam in the topsoil and a loamy sand texture in the subsoil (Table 3). The acidification of the developed soils is pronounced, with pH-values in the topsoil generally between 3.0 and 4.0 (Table 4). The soils, especially the ones developed on the two moraines (S1 and S3), showed clear podzolisation features (Tables 3 – 5) with a distinct eluviation and illuviation of Fe, Al (selective extractions (Table 4) and total content (Table 5)) and partially soil organic matter (SOM), especially in the case of (S5). Except for S2, very high amounts of C_{org} (> 200, partly > 300 g kg^{-1}) were measured in the topsoils. Ortstein occurrence is pronounced in the Bsm horizon of S1. In the case of S2, only small fragments in the cm-range were found. Bulk density of the Bsm horizon (~ 1.75 g cm^{-3}) of S1 was estimated by measuring the volume of water that was displaced by dipping a piece

of ortstein in a water-filled pail (this only gives indicative values). Detailed investigations using SEM/EDS (Scanning Electron Microscope and Energy Dispersive Scanning) showed a porous nature of the Ortstein (data not shown). Coatings consisted of Fe- and Al-oxyhydroxides, clays and organic matter. On the outer border of the Ortstein, Fe is accumulated. Formation of the Ortstein is due to intense eluviation of Fe, Al and subsequent formation of aggregates in the Bs horizon.

Oxalate- and dithionite-extractable amounts of Fe, Al and Si are presented in Table 4. The podzolisation process is clearly represented by high concentrations of Fe and Al in the Bs and Bhs horizons. Especially in the case of Al and Si, the oxalate-extractable part is higher than the dithionite-extractable one, which indicates the presence of imogolite-type materials. In some cases, especially in the Bs or BC horizon where an enrichment of Fe was found, Fe_o and Fe_d showed the same concentration. In the profiles S2 and S3, the concentration of Fe_o was even slightly higher than Fe_d. Fe_o exceeds Fe_d only in the presence of crystalline magnetite, which is dissolved by oxalate instead of dithionite (Lorenzoni et al., 1995).

4.2. Mass balance calculations, weathering indexes

Assuming an increasing element loss with increasing age (a more mature weathering state of the soil), the following order of elemental losses can be expected: Daun moraine > Egesen moraine > rock glacier with increasing values from the front to the rooting zone (starting zone within a former moraine). Figure 3 shows that our assumption was confirmed by the findings. The element loss patterns of Si, Al, Na and K show a good representation of the expected trend based on the morphostratigraphy. A striking phenomenon was the chemical behaviour of the soil of the rock glacier front (dark grey bar in Fig. 3). Except for the element K, the calculated element losses values were too low and did not fit into the coherent trend.

The molar ratio of (K+Ca)/Ti is used as a dating method for rock varnish in semi-arid to arid regions (Harrington and Whitney, 1987). As Ti is considered to be an immobile element, the ratio can

295 be used as a weathering index: the lower it is, the higher the degree of weathering. The (K+Ca)/Ti
296 ratio in the topsoil horizons (O, OE, E) showed a temporal trend tending to an asymptotic value
297 (Fig. 4). A significant part of K and Ca is leached with time leading to a passive enrichment of Ti.
298 A linear trend was obtained using the index *B* (Kronberg and Nesbitt, 1981) (Fig. 4). According to
299 this index, an enrichment of Al over Ca, K and Na occurs with time. On the basis of this index, a
300 good differentiation of the sites was obtained.
301
302 *4.3. Main mineralogy*
303 Results of the AutoQuan analyses give an overview of the main mineralogical composition. De-
304 tailed analyses of the clay fraction are not possible using this approach due to the presence of inter-
305 stratified and irregular transition structures. With AutoQuan, the mean concentration of primary
306 minerals in the sand (2000 – 63 µm), silt (63 – 2 µm) and clay fraction (< 2 µm) of the parent mate-
307 rial could be derived (Table 6). The variability of minerals found in all these fractions is very low
308 which confirms the uniformity of the parent material at all sites. Typically, the sand and silt frac-
309 tions were dominated by plagioclase, K-feldspar (microcline) and quartz. With decreasing particle
310 size the proportion of phyllosilicates (mica and chlorite) increased. The clay fraction consisted pre-
311 dominantly of sheet silicates (about 60%). Traces of calcite (close to the detection limit) seem to be
312 present in the sand and silt fraction.
313 With time, the proportion of more-easily weatherable minerals such as plagioclase, epidote and
314 chlorite distinctly decreased in all fractions of the topsoil (Fig. 5). Although a trend could be meas-
315 ured, it did not in most cases really tally with the expected one (according to the dated surface
316 ages). A good differentiation with this technique is rather difficult. The soil on the Daun moraine
317 could be distinguished more or less from the soil on the Egesen moraine. The sites on the rock gla-
318 cier, however, showed a rather fuzzy picture.
319

320 *4.4. Clay mineralogy*

321 X-ray diffraction patterns of the clay fraction for typical soil horizons are presented in Figure 6. The
322 X-ray diffractograms of all C or BC horizons were similar. XRD patterns of the Mg-saturated sam-
323 ples showed three fundamental reflections at 1.40, 1.00 and 0.71 nm (Fig. 6). The peak at 1.00 is
324 indicative of mica. K-saturation only slightly changed the XRD pattern. The subsequent heating at
325 335 °C and 550 °C allowed the identification of hydroxy-interlayered vermiculite (HIV) and chlo-
326 rite. No kaolinite could be detected with infrared analyses. Thus, the peak in the XRD pattern at 1.4
327 nm (Mg-saturation) represents Fe-rich chlorite with a very intense d(002*) reflection at 0.71 nm
328 (Moore and Reynolds, 1997). A further minor peak was detectable at 1.20 nm (Mg-saturated and
329 EG-solvated sample) showing an interstratification of mica with HIV.

330 In general, in the Bs horizon (and similarly also Bsm) of the investigated sites, the proportion of the
331 interstratified mineral mica-HIV as well as HIV itself strongly increased. Furthermore, a minor
332 amount of a second mica-HIV population formed (1.10 nm; Mg-saturated or EG-solvated sample).
333 Some kaolinite could be detected with IR (data not shown). The XRD pattern of the OE horizon of
334 the lower part of the rock glacier was very much disturbed by the presence of poorly crystalline
335 oxyhydroxide phases. Nonetheless, the main mineral phases were recognisable. Besides mica, a
336 new expandable phase using EG is appearing (smectite). Furthermore, a regularly-interstratified
337 mineral with a partially EG expandable phase exists that could be identified by the shift of the peak
338 at 2.39 nm (Mg-saturated) to 2.60 nm (EG-solvated). Consequently, some mica is interstratified
339 with smectite (or vermiculite) (with d(001*) and d(002*) at 2.39 and 1.21 nm, respectively, in the
340 Mg-saturated state that would correspond to a mica/smectite or mica/vermiculite ratio of approxi-
341 mately 60/40 (Moore and Reynolds, 1997). Smectite was recognised by the peak at 1.64 nm after
342 EG solvation. Chlorite does not exist anymore in this sample.

343 The XRD patterns of the E horizon of the Egesen moraine showed similarities to the E horizon of
344 the soil in the upper part of the rock glacier. In both samples a relatively high proportion of a regu-

345 larly-interstratified mica-smectite could be discerned. No chlorite was present. Kaolinite could be
346 identified by IR-analyses. Mica and some HIV (or HIS) were present in these samples. The highest
347 amount of smectite could be clearly detected in the E horizon of the Daun moraine (distinct peak at
348 1.64 nm; EG-solvated sample). Kaolinite was identified using IR and XRD (d(001) peak at 0.71
349 nm). Also in this sample, a regularly-interstratified mica-smectite could be detected.
350 In order to check the presence of hydroxy-interlayered smectite (HIS), samples that potentially con-
351 tain HIS were treated with sodium citrate (Fig. 7). An enlarged peak at 1.65 nm after ethylene gly-
352 col saturation and a more pronounced collapse towards 1.0 nm after K-saturation compared to the
353 untreated samples are characteristic for the presence of HIS. Based on that, HIS could be identified
354 in the E and OE horizons of the upper and middle part of the rock glacier as well as in the E horizon
355 of the soil developed on the Egesen moraine. In all other samples, no indications about a possible
356 presence of HIS were obtained.
357 XRD measurements in the range between 58° and 64° 2θ on powder samples provide information
358 about the presence of di- and trioctahedral minerals, respectively (data not shown). In all profiles,
359 dioctahedral mineral gained in importance with an increasing degree of weathering (from the C/BC
360 to the E/OE horizons). This went along with a reduction of trioctahedral species. Consequently,
361 main phyllosilicate transformation could be seen within the dioctahedral and trioctahedral distribu-
362 tion. Dioctahedral smectite formed at the expense of trioctahedral mica and chlorite.
363 The distribution of phyllosilicates for the E/OE horizons and selected C/BC horizons are summa-
364 rised in Figure 8. The latter ones were mainly characterised by chlorite and mica. For the C horizon
365 of the Daun moraine profile, a considerable amount of mica-HIV could be determined. The BC ho-
366 rizon of the Egesen moraine contained around 20% HIV.
367 Regarding the topsoil, the E horizon of the Daun moraine had by far the highest smectite content,
368 followed by the middle and lower part of the rock glacier and the Egesen moraine. The upper part
369 of the rock glacier showed only a low content of smectite, whereas a very high amount of smectite-

mica could be detected. The E horizon of the Daun moraine showed high concentrations of mica-HIV but no vermiculite and only a low concentration of kaolinite. Some vermiculite could only be found in the middle part of the rock glacier. Compared to the C/BC horizons, the relative loss of chlorite and mica suggests that their alteration is the main source for the formation of secondary clays like smectite.

5. Discussion

Mass balance calculations, weathering index (index B) and the (K+Ca)/Ti ratio all indicate that significant leaching losses of major base cations has occurred (Figs 3 and 4). These losses led to a corresponding passive enrichment of Al or Fe (Martínez Cortizas et al., 2003). The (K+Ca)/Ti ratio reflects the situation in the topsoils (O, OE and E horizons). As this ratio also includes here both the fine earth and the soil skeleton, it is less affected by external influences (such as pedoturbation; see below). The weathering index B shows a clear time-trend. This type of trend is also known from other investigation areas (Egli et al., 2008). Our results demonstrate that base cation leaching was the dominant process over the whole observation period. If almost no disturbances — such as erosion, deposition (or 'upbuilding' according to Johnson et al. (1990), pedoturbation — occurred during the life-time of a soil, chronosequences may give indications about rates of pedogenic processes (for an overview see Costantini et al., 2009).

A chemical mass balance can be influenced and disturbed by aeolian inputs. The influence of loess deposits can be inferred by the quantity of silt in the soil and its mineralogical composition. The dominant minerals in loess are usually quartz (Ollier, 1969; Bronger and Heinkele, 1989), mica and kaolinite. Although there was a decrease of quartz with increasing soil depth, aeolian deposits could not directly be inferred from these findings, as a relative enrichment of quartz can also be due to weathering. The grain size distribution of the soil did not reveal a major aeolian input. Kaolinite

395 could be found in the clay fraction of the surface and also subsurface horizons. This rather indicates
396 an active formation of kaolinite. The origin of kaolinite (Fig. 6; 0.71 nm in the E horizon) can pre-
397 sumably be traced back to the weathering of plagioclase. Traces of kaolinite (close to the detection
398 limit; identified using AutoQuan) could also be detected in the silt fraction of some surface soil ho-
399 rizons. Consequently, some minor aeolian inputs seem to have occurred.
400 It has been repeatedly shown that clay minerals' composition in soils is a valuable tool to investi-
401 gate chronosequences and to derive environmental conditions (e.g. Harris et al., 1980; Righi et al,
402 1999; Shaw et al., 2010). Smectite constitutes an end-product of mica and chlorite alteration (Righi
403 et al., 1999; Egli et al., 2003). In the surface horizons of podzolic soils, smectites developed either
404 from chlorite (Mg- and Fe-rich with a clinochlore-chamosite character; Egli et al., 2003) through
405 the removal of hydroxyl-interlayers or from trioctahedral mica, which weathers in a first step to
406 regularly or irregularly interstratified 2:1 clay minerals. Therefore, the amount of smectite is posi-
407 tively correlated with the weathering state and — given that formation factors other than time are
408 comparable for the studied soils — the age of a soil. From this point of view, the soil developed on
409 the Daun moraine can be identified as the oldest (Fig. 6). Within the relict rock glacier, a meaning-
410 ful picture can be drawn with more-weathered soils in the lower and middle part and a less-
411 developed profile in the upper part. The clay mineral composition of the lower and middle part of
412 the relict rock glacier reflects properties that would indicate more developed soils than the Egesen
413 moraine. This disagrees with the stratigraphic setting and points to the presence of some pre-
414 weathered material that was integrated into these soils (due to pedoturbation; see also below). This
415 is also partially shown by the mass balance calculations where the site at the rock glacier front does
416 not fully fit into the general sequence (Fig. 3).
417 The investigated chronosequence contains a soil series of 0 to 15 kyr. However, no data point be-
418 tween 0 and 8 kyr is available. Alpine glaciers have varied during the last 10000 years near the bor-
419 ders of the moraines of the year 1850 (Patzelt, 1977; Maisch, 1992). This fact makes it difficult to

420 find sites in the Alps with an undisturbed soil development for the weathering period between 0 and
421 10000 years (Egli et al., 2001). The curves computed by means of specific regression models lack,
422 therefore, data for this period of soil development. The obtained regression functions have conse-
423 quently a remaining speculative character. Furthermore, soil evolution in the observed time-span is
424 influenced by minor inhomogeneities of the parent material and variations of the climate (and sub-
425 sequently of the vegetation) which is discussed below.
426 A chronosequence for several pedosignatures could be observed. Some of these trends seem, how-
427 ever, to be rather fuzzy. This fuzziness is due to the soils that developed on the rock glacier. The
428 source material at an initial stage of the rock glacier formation was most likely provided by the
429 Egesen moraine, back-filled sediments and eventually also by material from a former Daun moraine
430 (Maisch, 1981). An inhomogeneous and repeatedly reworked composition, possibly accompanied
431 by the incorporation of pre-weathered material, may adulterate the signal and lead to results that are
432 difficult to interpret. Dorji et al. (2009) found that the detailed picture of a chronosequence can be
433 complicated by minor localised reversals of these trends. It may be that local backfilling and post-
434 incision additions of soil parent material facilitated the persistence of minor peculiarities and appar-
435 ent inconsistencies. An additional disturbing factor is a high proportion of coarse material. This was
436 typical especially for the profiles on the rock glacier with skeleton weight percentages of > 70 %
437 (Table 3). This hampers the formation of a well-pronounced pedogenic horizontation (Schaetzl,
438 1991). Compared to the more homogenous composition of the two moraines, dislocation processes
439 in the soils developed on the relict rock glacier more often follow preferential paths, for instance
440 along the surfaces of boulders.
441 This situation shows that disturbing factors like redistribution processes and pre-weathering must be
442 taken into account when using soils as relative age indicators (Caspari, 2007). Although established
443 as a tool for estimating the relative ages of Quaternary deposits (e.g. Birkeland, 1999; Zech et al.,

444 2003), soil development data should thus be applied in combination with other relative and/or nu-
445 merical age data.
446 Pedogenesis through the observed time frame has not been continuous and completely similar for
447 all sites (Fig. 9). The soil at site S1 started its formation earlier (after the Oldest Dryas) and experi-
448 enced in the Younger Dryas a cooler climate than during the Holocene. Since the Holocene, all soil
449 had similar climatic conditions. These minor differences (between S1 and S2-S5) may have also
450 influenced the measured trends. Frauenfelder et al. (2001) estimated the differences in mean annual
451 air temperature between the Younger Dryas period and today using the topographic position of 32
452 relict rock glaciers in the Err-Julier area (Swiss Alps) and, therefore, close to the Albula region.
453 Their results suggest that mean annual air temperature during the Younger Dryas was c. 3 - 4 °C
454 lower than modern values ($\Delta T = T_p - T_f$; with T_p = present day mean annual temperature and T_p =
455 former mean annual temperature) and that the lower limit of permafrost was depressed considerably
456 more than the glacier equilibrium lines. This indicates drier conditions than today. The present-day
457 limit of permafrost at north-facing sites varies is in the range 2400 to 2600 m asl depending on the
458 topography (FOEN, 2005). In the Younger Dryas, permafrost had been present in areas above c.
459 1950 m asl in slopes exposed to north, above 2200 m asl in easterly exposed areas, above 2450 m
460 asl on south-faced slopes and above 2150 m asl in west-exposed slopes (i.e. 500 m to 600 m below
461 the present-day limits of discontinuous permafrost; Frauenfelder, 2001; FOEN, 2005; Böhlert et al.,
462 2011). In the Preboreal, conditions became established that were similar to those of the present-day
463 but during the Older Atlanticum (c. 8000 – 5000 y BP) warmer conditions prevailed ('climatic op-
464 timum'). In an earlier work, palynological investigations were carried out at a nearby peat bog
465 (Crap Alv; Burga in Maisch, 1981). These analyses revealed that a re-forestation occurred shortly
466 after 10550 – 11400 cal yr BP (Maisch, 1981; Böhlert et al., 2011). In the Boreal, a Larch-Swiss
467 stone pine (*Pinus cembra*) forest established. In the Older Atlanticum (c. 8 ky BP), Norway spruce
468 immigrated into this region. During the climate optimum, the extension of Norway spruce (*Picea*

abies) reached a maximum at the expense of the Swiss stone pine/mountain pine forest. After this warm phase, the climatic situation remained similar to that of now and the proportion of *Picea abies* decreased. All these variations (climate, vegetation) finally affected soil evolution to a certain degree. The environmental conditions for all soils were identical for the last 8.6 ky. The oldest soil, however, started its development in a slightly colder climatic phase.

The mineralogical and chemical composition of the granitic till ('Julier granite') is homogeneous. All sites had a high soil skeleton proportion in the parent material. It is known from other studies that even minor physical variations in finer grained material may accelerate or retard chemical weathering (e.g. Egli et al., 2002). Phillips (2001) stated that pedogenesis is marked by divergence, whereby differences in initial conditions or local perturbations persist and increase to produce a more variable soil cover. This statement is, however, based on a more landscape-based view.

The study of long-term soil and weathering mechanism signals has, by necessity, to cope with such inconveniences (as only natural archives – among which soils can also be listed – can give an insight into long-term processes). Although soil evolution was not perfectly continuous and some inhomogeneity of the parent material must be taken into account, the established sequences are meaningful and reflect the geomorphic settings surprisingly well. According to Johnson et al. (1990), soil genesis can be viewed in a comprehensive framework of soil evolution that consists in developmental and even regressive pathways.

The selected parameters (mass balance, weathering indexes and clay mineralogy) traced the evolution astonishingly far back and in most cases a relative age separation was possible. Furthermore, these parameters enabled an additional insight into evolutionary processes of the investigated sites.

6. Conclusions

We studied soil formation as an age proxy for the period during the transition of the Lateglacial to the Holocene. The soils have an age of 8.6 to 14.9 ky. As relative measures for soil age, soil mineralogy with a main emphasis on the clay fraction, weathering indexes and mass balance calculations were applied. We obtained the following main findings:

- Although climatic conditions (and consequently also vegetation) were not always completely identical during soil formation (colder climate at the start of soil formation of the oldest soils), typical, pedogenetic trends could be detected.
- Weathering indexes such as the (K+Ca)/Ti ratio or the B-index reflect reasonably well a time trend. These ratios refer to the topsoil horizons (including O, OE and E horizon) and include the fine earth as well as the soil skeleton fraction and are not so easily affected by a possible pedoturbation.
- The mineralogical composition and the mass balance approach yielded a partially inconsistent picture. Some main features can be repeatedly recognised using the different methods. In most cases, the Daun moraine could clearly be identified as the oldest of the investigated landforms. A valuable separation from the Egesen moraine was, thus, possible. The soils developed on the rock glacier posed, however, some problems. The approaches used suggest the presence of pre-weathered material, which influenced the mineralogical and chemical characteristics of the soils developed on the relict rock glacier.
- Soil clay mineralogy and chemical mass balances consequently are sensitive methods to discover disruptive factors that affect the time trends.
- Techniques that include several soil horizons such as the (K+Ca)/Ti ratio, the B-index and the mass balance approach gave more meaningful results (in terms of the expected chronology) than the ones referring to single horizons (clay mineralogy). This would speak for reallocation processes within the soil profiles, without changing the overall characteristics of the soils.

- The combination of numerical dating and relative dating using soils enables an extended interpretation and mutual control. Such an approach ultimately leads to a better understanding of landscape reconstruction and evolution.

7. Acknowledgements

This research was supported by the Swiss National Science Foundation grants numbers 20-109565/1 and 20-124380. We are indebted to I. Woodhatch and B. Kägi for the support in the laboratory. We would like to thank R. Waldmeier and S. Heer for their support during sample collection in the field. We are, furthermore, indebted to Dr. Edoardo A.C. Costantini and an unknown reviewer for their helpful comments on an earlier version of the manuscript.

References

Alexander, E.B., Burt, R., 1996. Soil development on moraines of Mendenhall Glacier, southeast Alaska. 1. The moraines and soil morphology. Geoderma 72, 1–17.

Bearth P, Heierli H, Roesli F., 1987. Geologischer Atlas der Schweiz, Blatt 1237 Albulapass (Atlasblatt 81). Schweizerische Geologische Kommission und Landeshydrologie und –geologie, Bern.

Birkeland, P.W., 1999. Soils and geomorphology. 3rd edition, Oxford University Press, New York, 430 pp.

Böhlert, R., Egli, M., Maisch, M., Brandovà, D., Ivy-Ochs, S., Kubik, P.W., Haeberli, W., 2011. Application of a combination of dating techniques to reconstruct the Lateglacial and early Holocene landscape history of the Albula region (eastern Switzerland). Geomorphology, doi:10.1016/j.geomorph.2010.10.034.

542 Brimhall, G.H., Dietrich, W.E., 1987. Constitutive mass balance relations between chemical com-
543 position, volume, density, porosity, and strain in metasomatic hydrochemical sstems: results on
544 weathering and pedogenesis. Geochimica and Cosmochimica Acta 51, 567-587.
545 Bronger, A., Heinkele, T., 1989. Paleosol sequences as witnesses of Pleistocene climatic history. In:
546 Bronger, A., Catt, J.A. (Eds.), Paleopedology – Nature and Applications of Paleosols. Catena
547 Supplement 16, pp. 163-186.
548 Caspari, T., 2007. The soils of Buthan: parent materials, soil forming processes, and new insights
549 into the palaeclimate of the Eastern Himalayas. In: Kommission für Geomorphologie der Bay-
550 erischen Akademie der Wissenschaften (ed.), Relief, Boden, Klima (Band 22), Gebrüder Born-
551 traeger, Berlin/Stuttgart, pp. 1-128.
552 Chadwick, O.A., Brimhall, G.H., Hendricks, D.M., 1990. From a black to a grey box - A mass
553 balance interpretation of pedogenesis. Geomorphology 3, 369-390.
554 Corti, G, Ugolini, F.C., Agnelli, A., 1998. Classing the soil skeleton (greater than two millimeters):
555 Proposed approach and procedure. Soil Science Society of America Journal 62, 1620 – 1629.
556 Costantini, E.A.C., Makeev, A., Sauer, D., 2009. Recent developments and new frontiers in
557 paleopedology. Quaternary International 209, 1-5.
558 Dahms, D.E., 2004. Relative and numeric age data for pleistocene glacial deposits and diamictons
559 in and near Sinks Canyon, Wind River Range, Wyoming, U.S.A. Arctic, Antarctic, and Alpine
560 Research 36, 59-77.
561 Dorji, T., Caspari, T., Bäumler, R., Veldkamp, A., Jongmans, A., Tshering, K., Dorji, T., Baillie, I.,
562 2009. Soil development on Late Quaternary river terraces in a high montane valley in Bhutan,
563 Eastern Himalayas. Catena 78, 48-59.
564 EDI (Eidgenössisches Departement des Innern), 1992. Hydrologischer Atlas der Schweiz. Lande-
565 shydrologie und -geologie, Bern, Switzerland.

566 Egli, M., Fitze, F., 2000. Formulation of pedoligic mass balance based on immobile elements: a
567 revision. Soil Science 165 (5), 437-443.
568 Egli, M., Fitze, P., Mirabella, A,. 2001. Weathering and evolution of soils formed on granitic,
569 glacial deposits: results from chronosequences of Swiss alpine environments. Catena 45, 19-47.
570 Egli, M., Zanelli, R., Kahr, G., Mirabella, A. & Fitze, P. 2002. Soil evolution and development of
571 the clay mineral assemblage of a Podzol and Cambisol in "Meggerwald" (Switzerland). Clay
572 Minerals, 37, 351-366.
573 Egli, M., Mirabella, A., Fitze, P., 2003. Formation rates of smectites derived from two Holocene
574 chronosequences in the Swiss Alps. Geoderma 117, 81-98.
575 Egli, M., Mirabella, A., Nater, M., Alioth, L., Raimondi, S. 2008. Clay minerals, oxyhydroxide
576 formation, element leaching and humus development in volcanic soils. Geoderma, 143, 101-114.
577 Egli, M., Brandová, D., Böhlert, R. Favilli, F., Kubik, P., 2010. ^{10}Be inventories in Alpine soils and
578 their potential for dating land surfaces. Geomorphology 119, 62-73
579 Evans, D.J.A., 1999. A soil chronosequence from neoglacial moraines in western Norway. Geograf-
580 iska Annaler 81A, 47–62.
581 Fitze, P., 1982. Zur Relativdatierung von Moränen aus Sicht der Bodenentwicklung in den
582 kristallinen Zentralalpen. Catena 9, 265-306.
583 FOEN (Federal Office for the Environment), 2005. Hinweiskarte der potentiellen
584 Permafrostverbreitung in der Schweiz, Blatt Bergün 2005 (Map of the potential permafrost
585 distribution of Switzerland, map sheet Bergün 2005). Bundesamt für Umwelt BAFU, Bern.
586 Frauenfelder, R., Haeberli, W., Hoelzle, M., Maisch, M., 2001. Using relict rockglaciers in GIS-
587 based modelling to reconstruct Younger Dryas permafrost distribution patterns in the Err-Julier
588 area, Swiss Alps. Norsk Geografisk Tidsskrift 55, 195-202.
589 Gosse, J.C., Phillips, F.M., 2001. Terrestrial in situ produced cosmogenic nuclides: Theory and
590 application. Quaternary Science Reviews 20, 1475-1560.

591 Gross, G., Kerschner, H., Patzelt, G., 1977. Methodische Untersuchungen über die Schneegrenze in
592 alpinen Gletschergebieten. Zeitschrift für Gletscherkunde und Glazialgeologie 12, 223-251.
593 Harrington, C. D., Whitney, J. W., 1987. Scanning electron microscope method of rock-varnish dat-
594 ing. Geology 15, 967-970.
595 Harris, W.G., Iyengar, S.S., Zelazny, L.W., Parker, J.C., Lietzke, D.A., Edmonds, W.J., 1980. Min-
596 eralogy of a chronosequence formed in new river alluvium. Soil Science Society of America
597 Journal 51, 1673-1677.
598 Heuberger H. 1966. Gletschergeschichtliche Untersuchungen in den Zentralalpen zwischen Sellrain
599 und Ötztal. Wissenschaftliche Alpenvereinshefte 20. Universitätsverlag Wagner, Innsbruck.
600 Hitz, C., Egli, M., Fitze, P., 2002. Determination of the sampling volume for representative analysis
601 of alpine soils. Zeitschrift für Pflanzenernährung und Bodenkunde 165, 326-331.
602 Ivy-Ochs, S., Schäfer, J., Kubik, P.W., Synal, H.A., Schlüchter, C., 2004. The timing of
603 deglaciation on the northern Alpine foreland (Switzerland). Eclogae Geologicae Helvetiae 97,
604 47-55.
605 Ivy-Ochs, S., Kerschner, H., Reuther, A., Preusser, F., Heine, K., Maisch, M., Kubik, P.W.,
606 Schlüchter, C., 2008. Chronology of the last glacial cycle in the European Alps. Journal of
607 Quaternary Science 23 (6-7), 559-573.
608 Jenny, H. 1941., Factors of Soil Formation. McGraw-Hill, New York.
609 Johnson, D.L., Keller, E.A., Rockwell, T.K., 1990. Dynamic pedogenesis: Niew views on some key
610 soil concepts, and a model for interpreting Quaternary soils. Quaternray Research 33, 306-319.
611 Kahle, M., Kleber, M., Jahn, R., 2002. Review of XRD-based quantitative analyses of clay minerals
612 in soils: the suitability of mineral intensity factors. Geoderma 109, 191-205.
613 Keller, O., Krayss, E., 1993. The Rhine-Linth Glacier in the upper Würm: A model of the last
614 Alpine glaciation. Quaternary International 18, 15-27.

615 Kronberg, G.I., Nesbitt, H.W., 1981. Quantification of weathering of soil chemistry and soil fertil-
616 ity. Journal of Soil Science 32, 453-459.
617 Lal, D., 1988. In situ-produced cosmogenic isotopes in terrestrial rocks. Annual Review of Earth
618 and Planetary Sciences 16, 355-388.
619 Lanson, B., 1997. Decomposition of experimental X-ray diffraction patterns (profile fitting): a con-
620 venient way to study clay minerals. Clays and Clay Minerals 45, 132-146.
621 Lorenzoni P., Mirabella A., Bidini D., Lulli L., 1995. Soil Genesis on Trachytic and Leucitic Lavas
622 of Cimini Volcanic Complex (Latium-Italy). Geoderma 68, 79-99.
623 Maisch, M., Wipf, A., Denneler, B., Battaglia, J., Benz, C., 1999. Die Gletscher der Schweizer Al-
624 pen. Gletscherhochstand 1850, aktuelle Vergletscherung, Gletscherschwund- Szenarien.
625 Schlussbericht NFP 31 Projekt, vdf-Hochschulverlag ETH Zürich.
626 Maisch, M., 1992. Die Gletscher Graubündens: Rekonstruktion und Auswertung der Gletscher und
627 deren Veränderung sit dem Hochstand von 1850 im Gebiet der östlichen Schweizer Alpen
628 (Bündnerland und angrenzende Regionen). Schriftenreihe Physische Geographie 32, Universität
629 Zürich-Irchel, Switzerland.
630 Maisch, M., 1981. Glazialmorphologische und gletschergeschichtliche Untersuchungen im Gebiet
631 zwischen Landwasser- und Albulatal (Kt. Graubünden, Schweiz). Physische Geographie 3.
632 Furrer, G., Keller, W.A., Gamper, M., Suter, J. (Eds). Institute of Geography, University of
633 Zurich.
634 Martínez Cortizas, García-Rodeja Gayoso, E., Nóvao Muñoz, J.C., Pontevedra Pombal, X., Buur-
635 man, P., Terribile, F., 2003. Distribution of some selected major and trace elements in four Ital-
636 ian soils developed from the deposits of the Gauro and Vico vulcanoes. Geoderma 117, 215-224.
637 McKeague, J.A., Brydon, J.E., Miles, N.M., 1971. Differentiation of forms of extractable iron and
638 aluminium in soils. Soil Science Society of America Proceedings 35, 33-38.

639 Moore, D.M., Reynolds, Jr. R.C., 1997. X-ray diffraction and the identification and analysis of clay
640 minerals. 2nd edition, Oxford University Press, New York.
641 Munroe, J.S., 2008. Alpine soils on Mount Mansfield, Vermont, USA: Pedology, history and in-
642 traregional comparison. Soil Science Society of America Journal 72, 524-533.
643 Ollier, C.D., 1969. Weathering. Oliver & Boyd, Edingburgh, Scotland.
644 Omotoso, O., McCarty, D. K., Kleeberg, R. and Hillier, S., 2006. Some successful approaches to
645 quantitative mineral analysis as revealed by the 3rd Reynolds cup contest. Clays and Clay Min-
646 erals 54, 748-760.
647 Parfitt, R.L., Childs, C.W., 1988. Estimation of forms of Fe and Al – a review, and analysis of
648 contrasting soils by dissolution and Mossbauer methods. Australian Journal of Soil Research 26,
649 121-144.
650 Parfitt, R.L., Childs, C.W., Eden, D.N., 1988. Ferrihydrite and allophane in four Andepts from
651 Hawaii and implications for their classification. Geoderma 41, 223-241
652 Patzelt, G., 1977. Der zeitliche Ablauf und das Ausmass postglazialer Kimaschwankungen in den
653 Alpen. In: Frenzel, B. (ed.), Dendrochronologie und postglaziale Klimaschwankungen in Eu-
654 ropa. Wiesbaden, Erdwissenschaftliche Forschung 13, pp. 248-259.
655 Penck, A., Brückner, E., 1909. Die Alpen im Eiszeitalter. 3 volumes, Leipzig, Tauchnitz.
656 Phillips, J.D., 2001. Divergent evolution and the spatial structure of soil landscape variability.
657 Catena 43, 101-113.
658 Plötze, M., Trausch Giudici, I. Messerklinger, S., Springman, S., 2003. Swiss Lacustrine Clay:
659 Mineralogical and mechanical characteristics. In: Vermeer, Schweiger, Karstunen, Cudny (eds.),
660 Int. Workshop on Geotechnics of Soft Soils-Theory and Practice, Noordwijkerhout, VGE, pp.
661 473-478.
662 Righi, D., Huber, K., Keller, C., 1999. Clay formation and podzol development from postglacial
663 moraines in Switzerland. Clay minerals 34, 319-332.

664 Rossi, A. M., Graham, R.C. 2010. Weathering and Porosity Formation in Subsoil Granitic Clasts,
665 Bishop Creek Moraines, California. Soil Science Society of America Journal 74, 172-185.
666 Schaetzl, R.J. 1991. A lithosequence of soils in extremely gravelly, dolomitic parent materials, Bois
667 Blanc Island, Lake Huron. Geoderma 48:305-320
668 Schaller, M., Blum, J.D., Ehlers, T.A., 2009. Combining cosmogenic nuclides and major elements
669 from moraine soil profiles to improve weathering rate estimates. Geomorphology 106, 198-205.
670 Shaw, J.N., Haek, B.F., Beck, J.M., 2010. Highly weathered mineralogy of select soils from South-
671 eastern U.S. Coastal Plain and Piedmont landscapes. Geoderma 154, 447-456.
672 Zech, W., Glaser, B., Abramowski, U., Dittmar, C., Kubik, P.W., 2003. Reconstruction of the late
673 quaternary glaciation of the Macha Khola valley (Gorkha Himal, Nepal) using relative and abso-
674 lute (^{14}C, ^{10}Be, dendrochronology) dating techniques. Quaternary Science Reviews 22, 2253-
675 2265.

Table 1
Click here to download Table: Table1.doc

Table1. General description of sampling sites and landform ages.

Site	Elevation (m a.s.l.)	Aspect (°N)	Slope (°)	Parent material	Vegetation	Land use	WRB (IUSS Working Group 2006)	Age of landform (ka)
S1	2100	35	11	Granite (Daun moraine; Oldest Dryas)	Larix decidua Pinus cembra Ericaceae	Natural forest Extensive pasturing possible	Umbric Podzol (Endoskeletic)	14.9 ± 1.8[1] 14.3 ± 2.3[2]
S2	2060	0	16	Granite (Lower rock glacier lobe)	Ericaceae Cladonia rangiferina	Natural alpine grassland, dwarf shrubs	Ortsteinic-Umbric Podzol (Episkeletic)	< 10.7 ± 0.9[1]
S3	2150	315	9	Granite (Egesen moraine; Younger Dryas)	Ericaceae	Natural alpine grassland, dwarf shrubs	Umbric Podzol (Endoskeletic)	10.7 ± 0.9[1]
S4	2130	300	8	Granite (Middle rock glacier lobe)	Ericaceae Cladonia rangiferina	Natural alpine grassland, dwarf shrubs	Umbric Podzol (Endoskeletic)	Age between S2 and S5[1]
S5	2280	300	6	Granite (Upper rock glacier lobe)	Ericaceae Cladonia rangiferina	Natural alpine grassland, dwarf shrubs	Albic Podzol (Endoskeletic)	8.6 ± 0.6[1]

[1]Böhlert et al., 2011; [2]Egli et al., 2010

Table 2
Click here to download Table: Table2.doc

Table 2. Chemical composition of the skeleton fraction of the parent material ('Albula granite').

Site	SiO_2 g/kg	Al_2O_3 g/kg	Fe_2O_3 g/kg	CaO g/kg	MgO g/kg	K_2O g/kg	Na_2O g/kg	MnO g/kg	P_2O_5 g/kg	TiO_2 g/kg	ZrO_2 g/kg	LOI g/kg
S1	670.8	149.3	38.4	25.0	12.6	23.1	31.0	0.79	1.24	5.01	0.21	25.1
S2	708.4	145.8	24.2	13.9	7.5	33.8	29.7	0.54	0.89	3.56	0.18	14.7
S3	696.6	152.5	30.2	12.8	11.8	31.8	31.3	0.58	0.95	4.38	0.24	18.6
S4	663.9	154.6	33.6	47.2	6.9	22.6	30.2	0.52	0.92	3.76	0.18	15.9
S5	691.6	141.8	27.8	15.8	9.4	32.6	26.6	0.58	0.88	3.75	0.17	17.4
Mean	686.3	148.8	30.9	22.9	9.6	28.8	29.8	0.60	0.98	4.09	0.20	18.3
SD	18.5	5.1	5.4	14.4	2.5	5.5	1.9	0.11	0.15	0.60	0.03	4.1

LOI = loss of ignition

Table 3
Click here to download Table: Table3.doc

Table 3. Some physical properties of the soils sampled in Val Mulix.

Site	Soil horizon	Depth (cm)	Munsell colour (moist)	Bulk density (g cm^{-3})	Skeleton[1)] (weight %)	Sand[2)] (g kg^{-1})	Silt (g kg^{-1})	Clay (g kg^{-1})
S1	O	0-13	5YR 1.7/1	0.37	3.1	502	386	112
	E	13-20	7.5YR 1.7/1	0.88	28.8	489	377	134
	Bhs	20-23	5YR 2/2	0.90	20.9	n.d.	n.d.	n.d.
	Bsm	23-50	5YR 3/4	1.75	60.9	823	154	23
	BC	50-70	10YR 5/4	1.68	53.2	n.d.	n.d.	n.d.
	C	>70	10YR 6/3	1.75	61.2	807	161	32
S2	OE	0-7	7.5YR 1.7/1	1.24	27.1	n.d.	n.d.	n.d.
	Bs	7-40	5YR 3/2	1.53	74.9	n.d.	n.d.	n.d.
	Bsm	40-60	7.5YR 4/4	n.d.	69.2	n.d.	n.d.	n.d.
	C	>60	10YR 4/4	1.93	78.9	n.d.	n.d.	n.d.
S3	O1	0-5	7.5YR 1.7/1	0.50	25.5	n.d.	n.d.	n.d.
	O2	5-10	10YR 2/2	0.49	17.0	494	369	137
	E	10-12	7.5YR 2/1	0.57	30.0	483	379	138
	Bhs	12-14	7.5YR 1.7/1	n.d.	27.1	n.d.	n.d.	n.d.
	Bs	14-26	5YR 3/4	0.81	50.1	793	181	26
	BC	26-60	10YR 4/6	1.36	67.9	814	154	32
S4	O	0-9	7.5YR 1.7/1	0.24	2.4	n.d.	n.d.	n.d.
	OE	9-18	7.5YR 1.7/1	0.40	5.8	n.d.	n.d.	n.d.
	Bs	18-30	5YR 2/3	1.32	56.6	n.d.	n.d.	n.d.
	BC	30-50	7.5YR 3/3	1.37	66.1	n.d.	n.d.	n.d.
	C	>50	10YR 4/4	1.51	75.3	n.d.	n.d.	n.d.
S5	O1	0-5	7.5YR 1.7/1		2.6	n.d.	n.d.	n.d.
	O2	5-10	7.5YR 1.7/1	0.33	12.4	n.d.	n.d.	n.d.
	E	10-15	7.5YR 4/2	0.70	36.5	n.d.	n.d.	n.d.
	Bhs	15-25	5YR 1.7/1	0.83	67.3	n.d.	n.d.	n.d.
	Bs	25-35	5YR 2/2	n.d.	64.3	n.d.	n.d.	n.d.
	BC	>35	10YR 3/4	1.54	72.5	n.d.	n.d.	n.d.

n.d.= not determined
[1)] Skeleton = Material > 2mm
[2)]Size fractions: Sand = 2000-63 µm; Silt = 63–2 µm; Clay = < 2 µm

Table 4
Click here to download Table: Table4.doc

Table 4. Chemical properties of the soils in Val Mulix.

Site	Soil horizon	Depth (cm)	pH ($CaCl_2$)	Org. C (g kg^{-1})	Total N (g kg^{-1})	C/N	Fe_t (g kg^{-1})	Si_o (g kg^{-1})	Al_o (g kg^{-1})	Fe_o (g kg^{-1})	Si_d (g kg^{-1})	Al_d (g kg^{-1})	Fe_d (g kg^{-1})
S1	O	0-13	2.7	202.8	8.6	24	7.23	n.d.	n.d.	n.d.	n.d.	n.d.	n.d.
	E	13-20	3.2	45.9	1.5	30	13.94	0.06	2.92	2.36	0.67	3.31	5.32
	Bhs	20-23	3.5	50.5	2.0	26	34.54	0.24	7.03	10.30	0.91	8.48	17.91
	Bsm	23-50	4.4	28.3	0.9	33	34.01	7.54	20.05	6.29	2.29	15.93	15.07
	BC	50-70	4.4	3.9	0.2	16	24.86	1.36	3.25	1.20	1.13	2.54	2.84
	C	>70	4.6	2.3	0.3	9	20.82	0.92	2.04	0.79	0.96	1.66	1.69
S2	OE	0-7	3.4	151.2	5.8	26	11.74	0.11	3.87	3.97	0.78	4.02	4.67
	Bs	7-40	4.3	17.7	0.4	41	18.74	2.33	8.37	3.05	1.40	6.22	3.52
	Bsm	40-60	4.2	43.4	1.1	38	19.24	6.29	17.89	5.79	1.77	10.32	5.44
	C	> 60	4.6	4.2	0.2	17	17.21	1.07	3.36	1.20	1.09	2.84	1.51
S3	O1	0-5	3.4	305.1	16.2	19	11.03	n.d.	n.d.	n.d.	n.d.	n.d.	n.d.
	O2	5-10	3.4	189.9	5.0	38	19.55	n.d.	n.d.	n.d.	n.d.	n.d.	n.d.
	E	10-12	3.4	95.3	2.6	36	23.46	0.15	5.44	5.12	0.66	6.10	6.98
	Bhs	12-14	3.8	94.9	3.1	31	20.25	0.18	15.18	10.71	0.75	14.35	10.07
	Bs	14-26	4.2	44.8	1.2	36	29.45	2.54	18.68	11.31	2.29	14.90	10.96
	BC	26-60	4.7	3.5	0.2	21	25.34	1.70	4.70	2.05	1.09	2.65	2.55
S4	O	0-9	3.1	278.3	12.0	23	5.97	n.d.	n.d.	n.d.	n.d.	n.d.	n.d.
	OE	9-18	3.3	171.3	6.0	29	13.35	0.01	3.99	3.03	0.61	3.85	5.16
	Bs	18-30	4.1	75.9	2.6	30	28.00	1.11	19.81	10.50	1.55	19.78	10.75
	BC	30-50	4.4	33.0	1.4	24	24.69	2.10	11.48	3.58	2.04	10.60	3.92
	C	> 50	4.5	11.3	0.5	22	22.72	1.19	5.01	1.36	1.24	4.94	1.98
S5	O1	0-5	3.3	328.6	14.3	23	7.20	n.d.	n.d.	n.d.	n.d.	n.d.	n.d.
	O2	5-10	3.4	240.1	8.4	29	9.60	n.d.	n.d.	n.d.	n.d.	n.d.	n.d.
	E	10-15	3.9	23.7	0.5	48	3.53	0.00	0.85	0.44	0.55	0.95	1.12

Bhs	15-25	4.1	88.2	3.4	26	28.73	0.51	11.89	10.03	1.10	12.82	12.12
Bs	25-35	4.6	46.3	1.4	33	30.62	2.15	14.53	8.00	1.83	12.21	8.25
BC	> 35	4.7	9.9	0.4	24	23.68	2.08	8.82	3.96	1.23	4.46	3.16

n.d. = not determined

Table 5
Click here to download Table: Table5.doc

Table 5. Concentrations of the main elements obtained by means of XRF. The values refer to the sum of earth and skeleton material (up to 10 cm in diameter).

Site	Soil horizon	Depth (cm)	OM* (g/kg)	CaO (g/kg)	MgO (g/kg)	K_2O (g/kg)	Na_2O (g/kg)	Al_2O_3 (g/kg)	Fe_2O_3 (g/kg)	SiO_2 (g/kg)	MnO (g/kg)	TiO_2 (g/kg)
S1	O	0-13	338.08	5.23	4.65	18.34	13.13	97.67	10.58	401.93	0.07	7.10
	E	13-20	56.22	9.33	7.58	27.23	20.32	147.22	21.77	594.84	0.20	7.70
	Bhs	20-23	68.75	13.92	10.95	23.79	21.69	149.20	47.87	552.81	0.39	7.13
	Bsm	23-50	19.01	22.57	13.36	21.60	27.84	158.45	43.25	622.90	0.68	5.30
	BC	50-70	3.14	19.65	11.32	29.36	27.75	149.77	31.60	680.39	0.56	4.34
	C	>70	1.51	15.33	9.14	29.32	29.73	145.26	25.34	701.68	0.55	3.77
S2	OE	0-7	189.56	8.22	4.67	28.03	20.92	124.13	16.49	562.41	0.15	4.68
	Bs	7-40	7.62	14.45	6.84	31.78	30.42	145.27	23.00	700.31	0.50	3.22
	Bsm	40-60	22.98	14.40	6.44	28.21	30.93	149.01	25.89	671.66	0.46	3.69
	C	>60	1.54	14.58	7.77	32.81	30.21	146.34	24.55	704.86	0.53	3.57
S3	O1	0-5	391.10	10.70	6.05	16.53	16.86	93.27	28.40	338.46	0.25	5.84
	O2	5-10	271.11	8.56	6.53	30.68	14.22	125.53	31.79	471.24	0.25	8.92
	E	10-12	114.70	19.06	8.63	32.44	17.10	157.43	41.58	508.00	0.46	10.84
	Bhs	12-14	118.86	10.76	5.52	28.90	18.96	155.07	30.81	488.83	0.23	6.17
	Bs	14-26	38.51	10.08	7.83	29.21	23.09	156.39	34.56	604.49	0.39	4.94
	BC	26-60	1.96	12.42	12.80	31.50	31.02	153.77	32.69	684.65	0.59	4.63
S4	O	0-9	467.35	5.38	3.00	12.82	12.49	64.38	8.82	273.46	0.01	4.75
	OE	9-18	277.52	8.79	5.18	22.69	15.33	121.63	19.70	446.10	0.09	7.71
	Bs	18-30	56.67	23.89	6.72	20.99	26.76	150.19	34.43	604.43	0.44	3.99
	BC	30-50	19.29	29.73	6.66	22.96	30.72	150.25	32.19	654.30	0.50	4.12
	C	>50	4.82	42.08	7.37	23.13	30.19	153.77	33.71	664.97	0.53	3.92
S5	O1	0-5	550.29	5.35	2.72	11.45	11.06	54.49	10.80	249.84	0.09	4.14
	O2	5-10	361.64	7.47	4.93	21.06	14.84	93.11	16.39	406.24	0.16	5.27

E	10-15	25.93	7.28	5.68	36.26	20.28	119.85	9.42	744.00	0.18	3.51
Bhs	15-25	49.63	12.35	7.01	33.43	24.87	140.06	29.15	640.74	0.45	4.15
Bs	25-35	28.42	16.16	8.71	29.30	27.11	147.64	35.00	624.61	0.53	4.44
BC	>35	4.69	15.77	9.51	31.74	26.44	144.07	29.91	680.00	0.56	3.96

*Organic matter = org C (fine earth and skeleton)*1.72

Table 6. Mean mineralogical composition of the parent material (C horizons of soils developed on the middle and lower part of the rock glacier, the Daun moraine and the BC horizon of the soil on the Egesen moraine) with respect to the sand, silt and clay fraction.

	Sand mean (wt.-%)	SD	Silt mean (wt.-%)	SD	Clay mean (wt.-%)	SD
Calcite	0.3	0.3	0.2	0.2	0.0	0.0
Chlorite	7.2	1.0	14.4	2.0	22.9	5.1
Epidote	4.4	2.8	7.5	5.1	3.4	1.2
Microcline	13.2	2.2	13.2	2.3	10.7	2.6
Mica	11.8	0.9	13.7	0.7	35.6	1.2
Na-Plagioclase	36.4	0.8	31.2	1.1	19.7	3.3
Quartz	26.8	1.6	19.8	2.6	7.8	1.4

SD = standard deviation

Figure captions

Fig. 1. Map with the geomorphologic situation based on Maisch (1981). The profiles investigated are indicated with S1-S5.

Fig. 2. Photographs of the profiles and their position in the investigation area. Except for S5 from the blocky upper part of the rock glacier, the soils show well-pronounced horizons which is especially true for the moraine profiles S1 and S3.

Fig. 3. Calculated mass balances (equation 5). The assumption is that the older the soils are, the higher are the element losses. Except for the profile near the rock glacier terminus (S2), the calculated mass losses are in accordance with the expected trend based on morphostratigraphy, namely for Si, Al, Na and K.

Fig. 4. Temporal evolution of the mean molar ratio of (K+Ca)/Ti and the weathering index *B* (equation 6) of the bulk material (fine earth and soil skeleton) in the topsoil (O, OE, E horizons). The initial value (t = 0) was calculated from the mean value of the C horizon of the sites.

Fig. 5. Relative proportion of easily weatherable minerals (plagioclase, epidote, chlorite) in the sand, silt and clay fraction (of the topsoil) as a funtion of time (mean values of the C horizons correspond to t = 0).

Fig. 6. XRD patterns of soil clays (< 2µm) of some selected horizons (C and B horizon; E or OE horizons). The XRD-curves were smoothed and corrected for Lorentz and polarization

factors. *d*-spacings are given in nm. EG = ethylene glycol solvation, Mg = Mg-saturation, K = K-saturation and corresponding heating treatments.

Fig. 7. XRD patterns soil clays of the OE horizon of site S4 (rock glacier middle part) before and after treatment with Na-citrate. The XRD-curves were corrected for Lorentz and polarization factors. *d*-spacings are given in nm. Treatment with Mg, Ethylene glycol (EG), K and heating to 335 °C and 550 °C, respectively, leads to diagnostic peaks as a result of clay-type specific expansion and contraction behaviour (1). Important *d*-spacings are given in nm. After citrate treatment, the more pronounced peak at 1.65 nm after EG solvation (2) and the greatly improved collapse after K saturation (3) evidence the presence of HIS (hydroxy-interlayered smectite).

Fig. 8. Results of the semi-quantitative analysis of the clay fraction, in each case for the most weathered horizon (E/OE). As a reference, the C and BC horizons of the moraines are shown as well. Taking the amount of smectite as an age indicator, the Daun moraine shows clearly the highest degree of development. The middle and lower part of the rock glacier have a surprisingly high amount of smectite while in the upper part no smectite at all is detected. The C and BC horizons are characterised by a high amount of chlorite.

Fig. 9. Soil formation through time (given by the black columns) in view of the climate history in the investigation area. Climatic indications are given by the glacier variations and the pollen chronozones. In view of the climate, S2 – S5 had similar conditions. The evolution of soil S1 started earlier and partially developed in the Younger Dryas (cooler climate).

Figure 1

Click here to download high resolution image

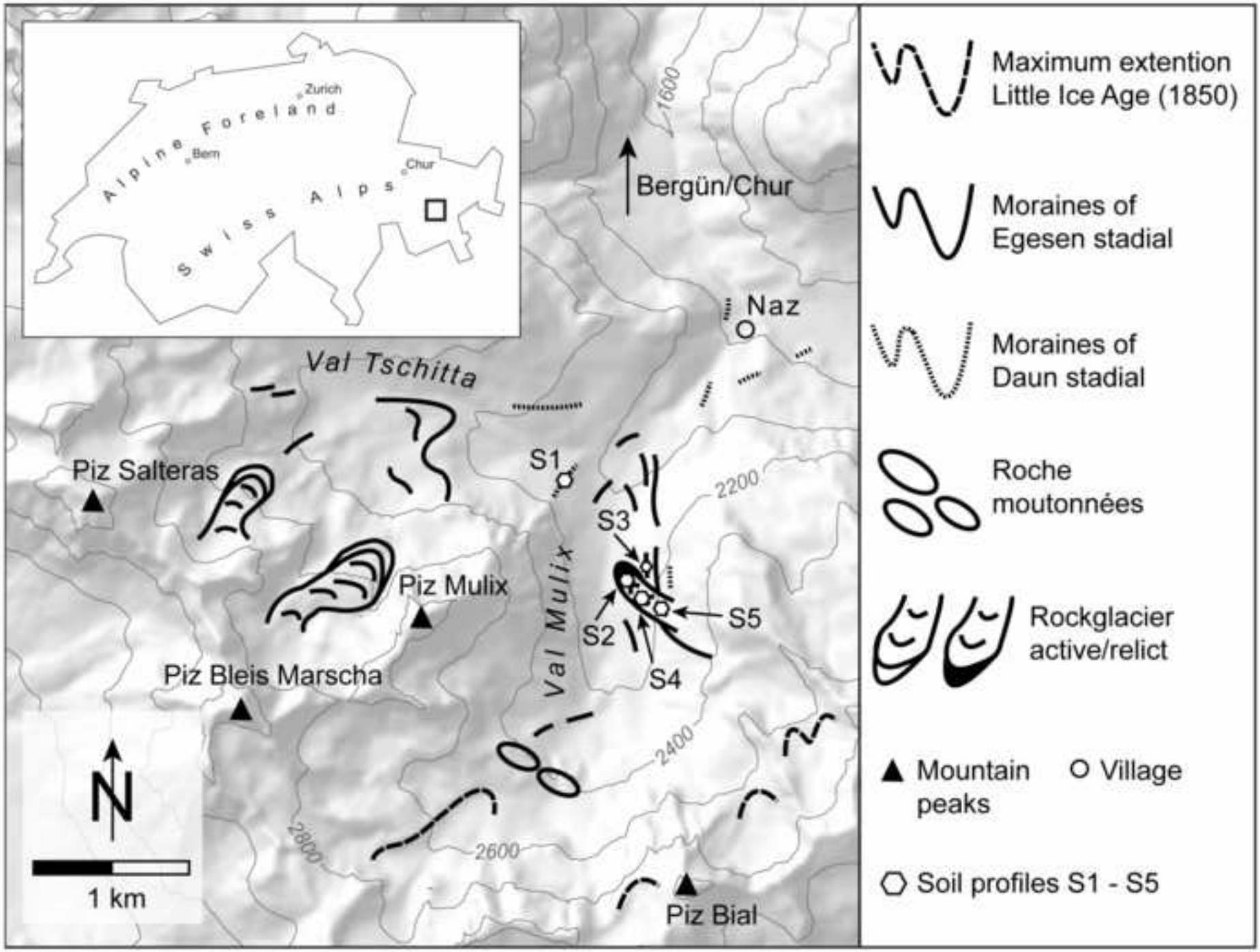

Figure 2

Click here to download high resolution image

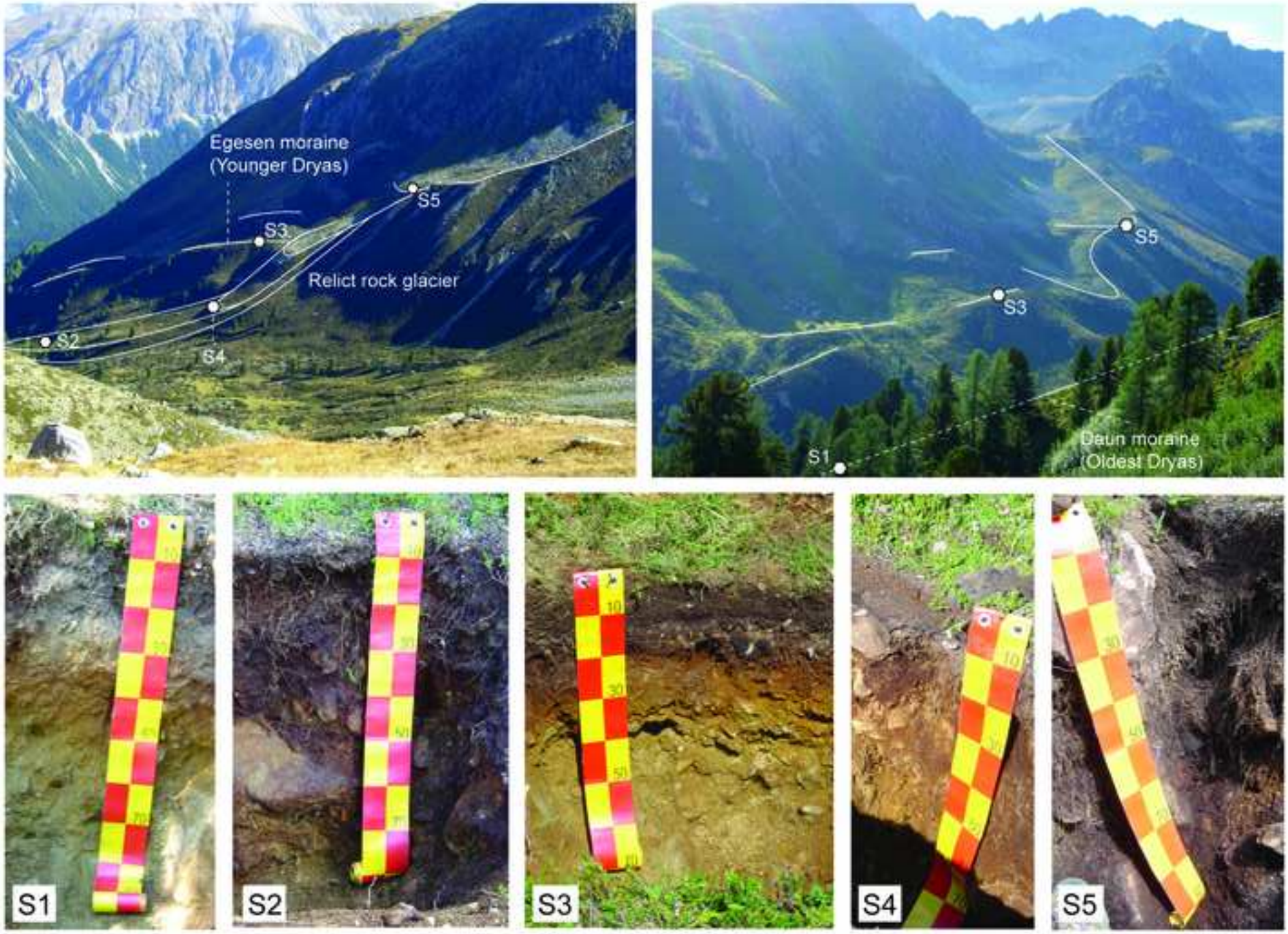

Figure 3

Click here to download high resolution image

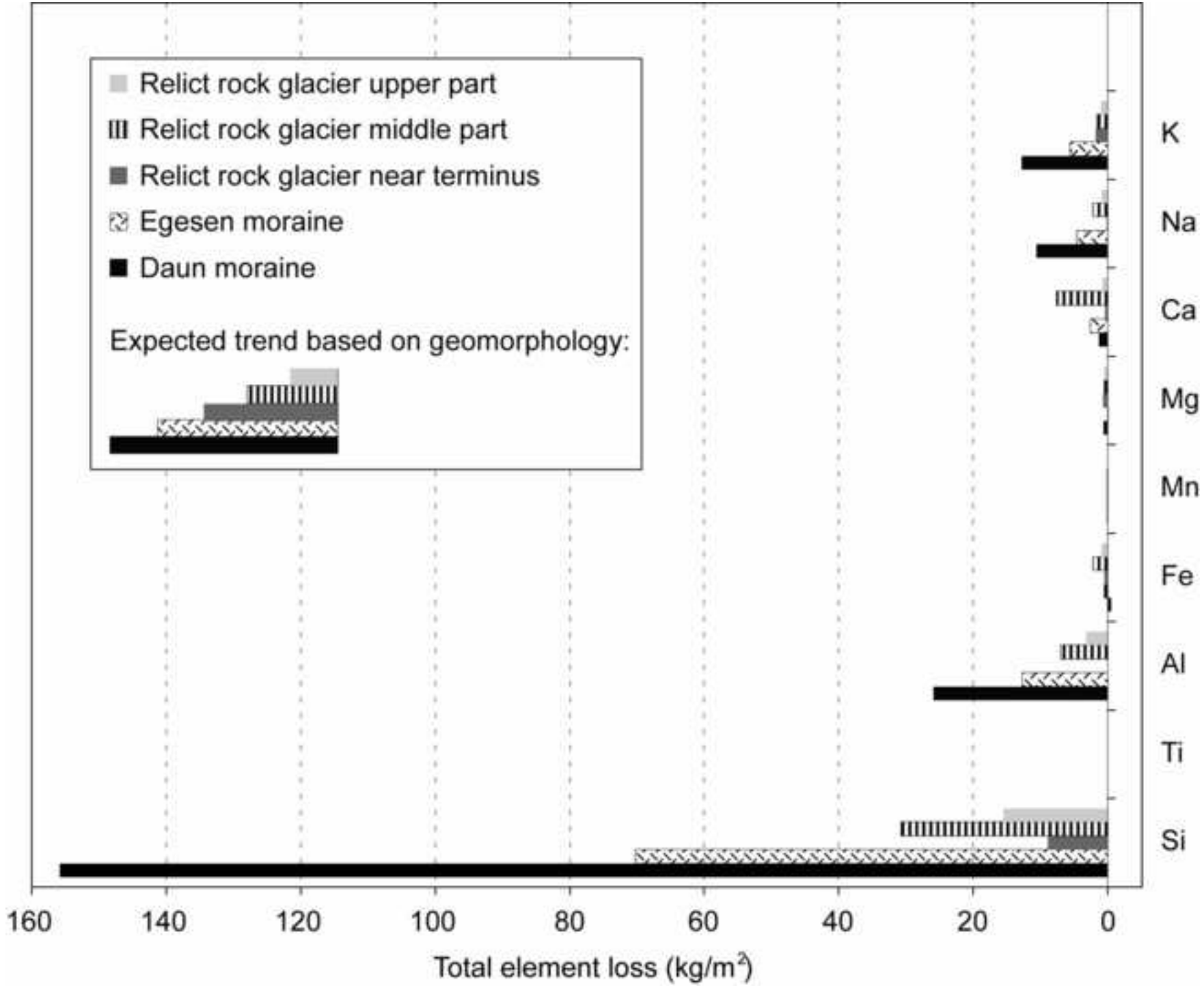

Figure 4

Click here to download high resolution image

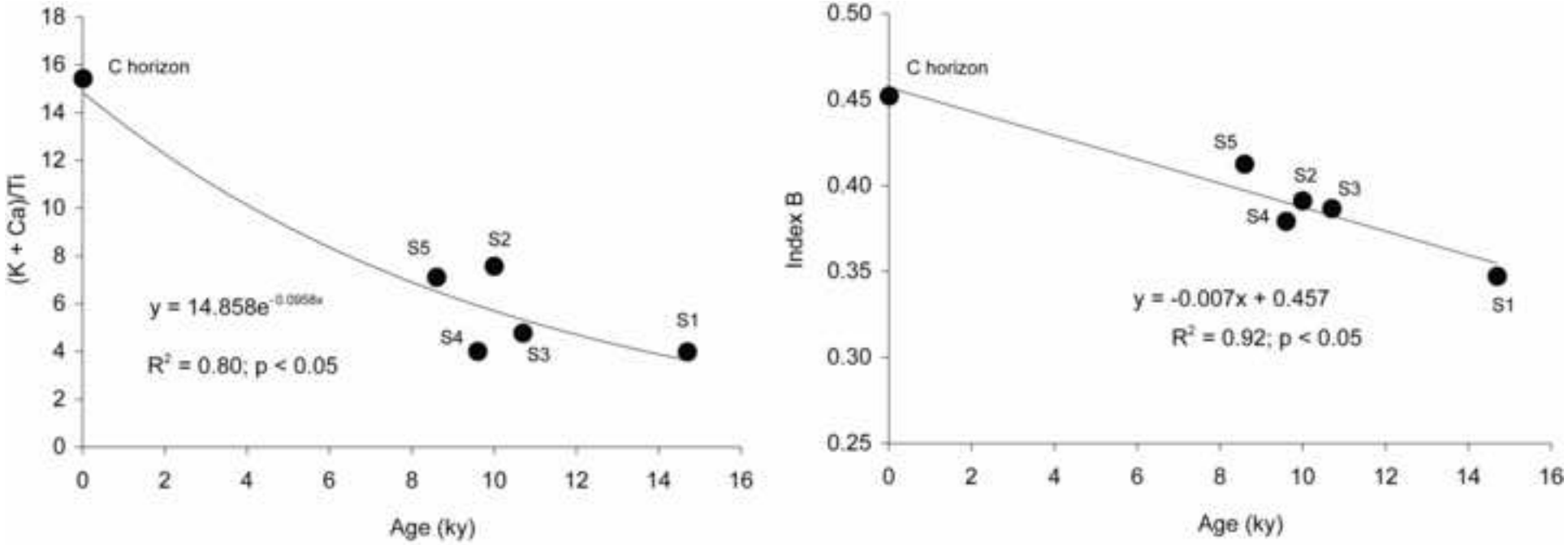

Figure 5

Click here to download high resolution image

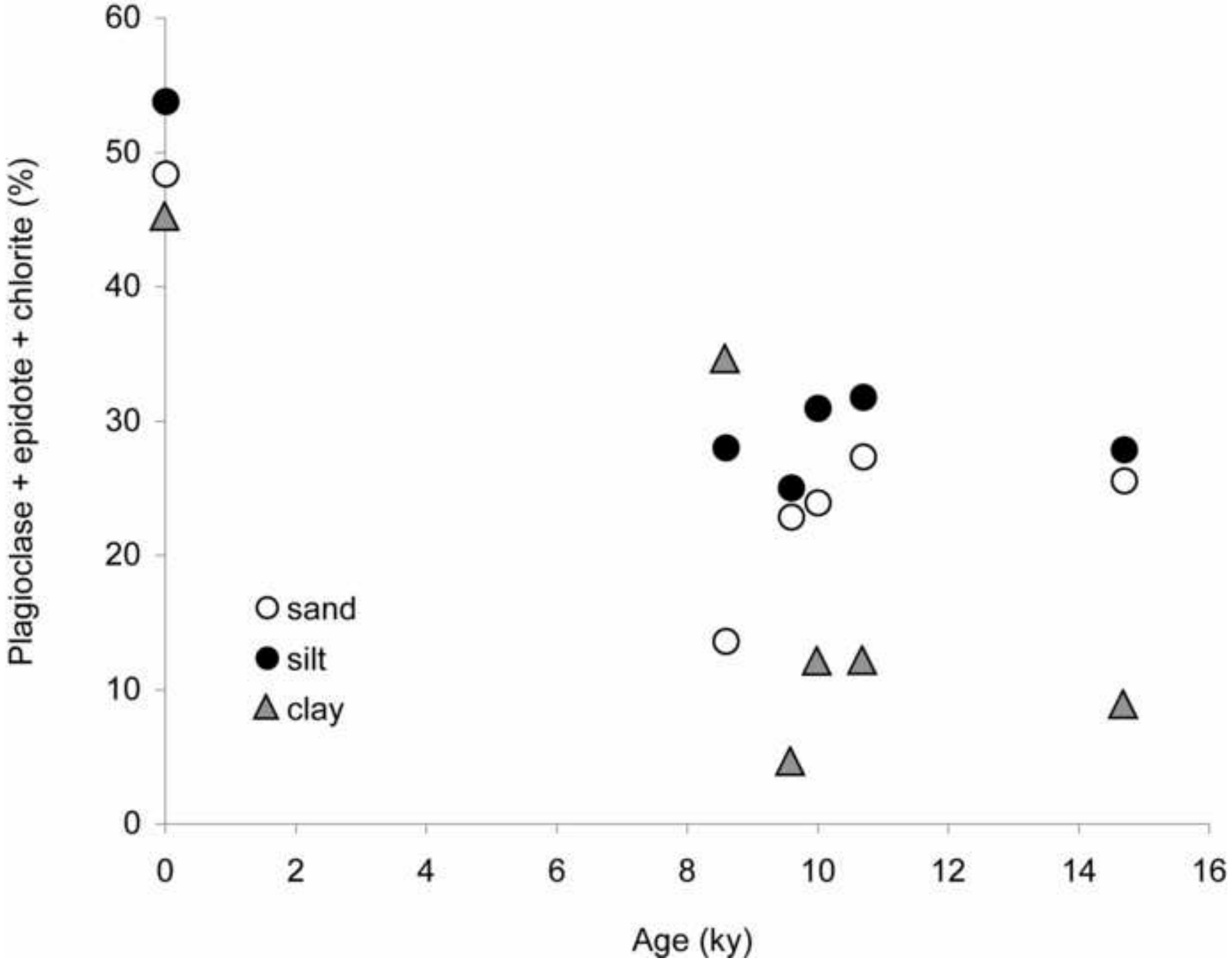

Figure 6

Click here to download high resolution image

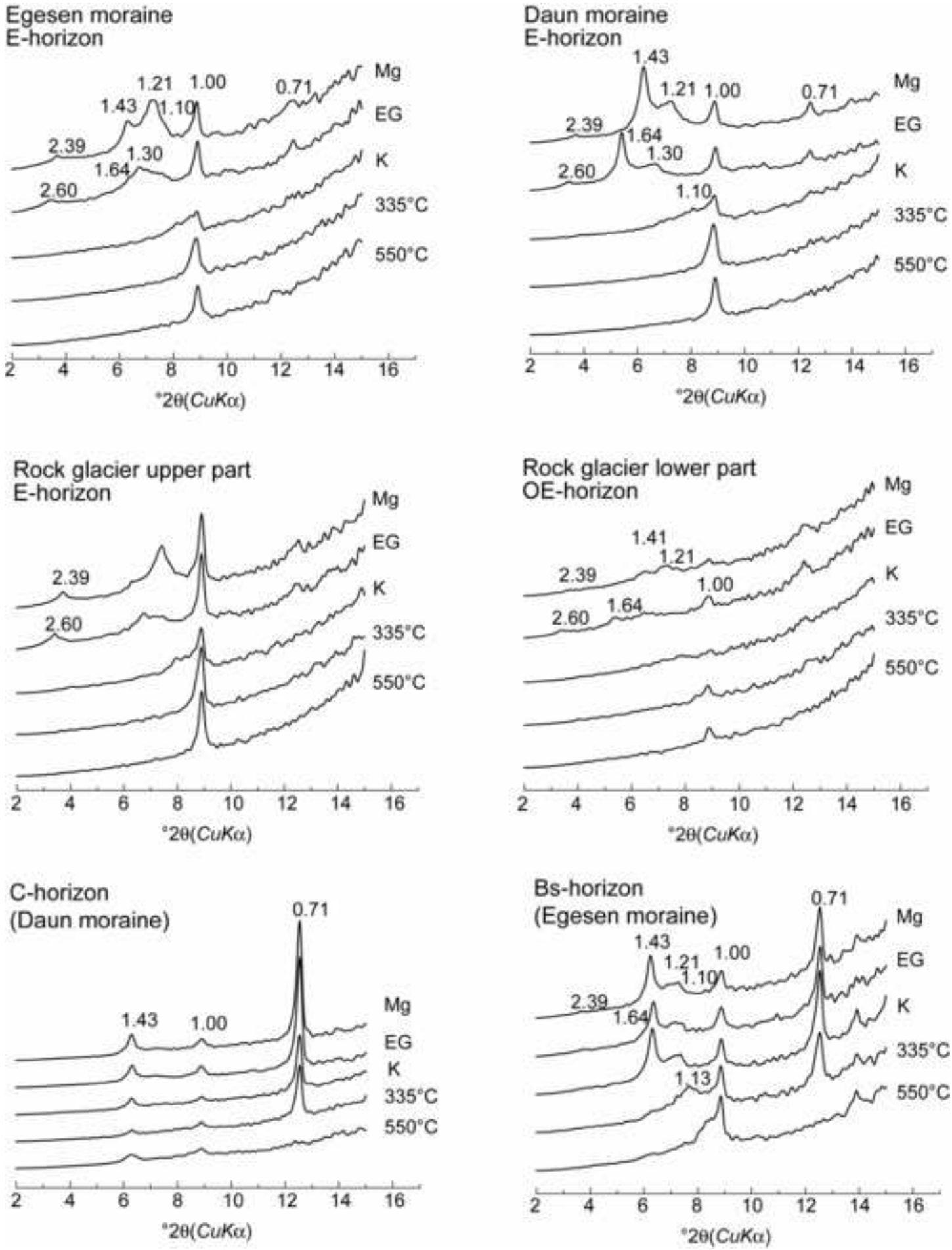

Figure 7
Click here to download high resolution image

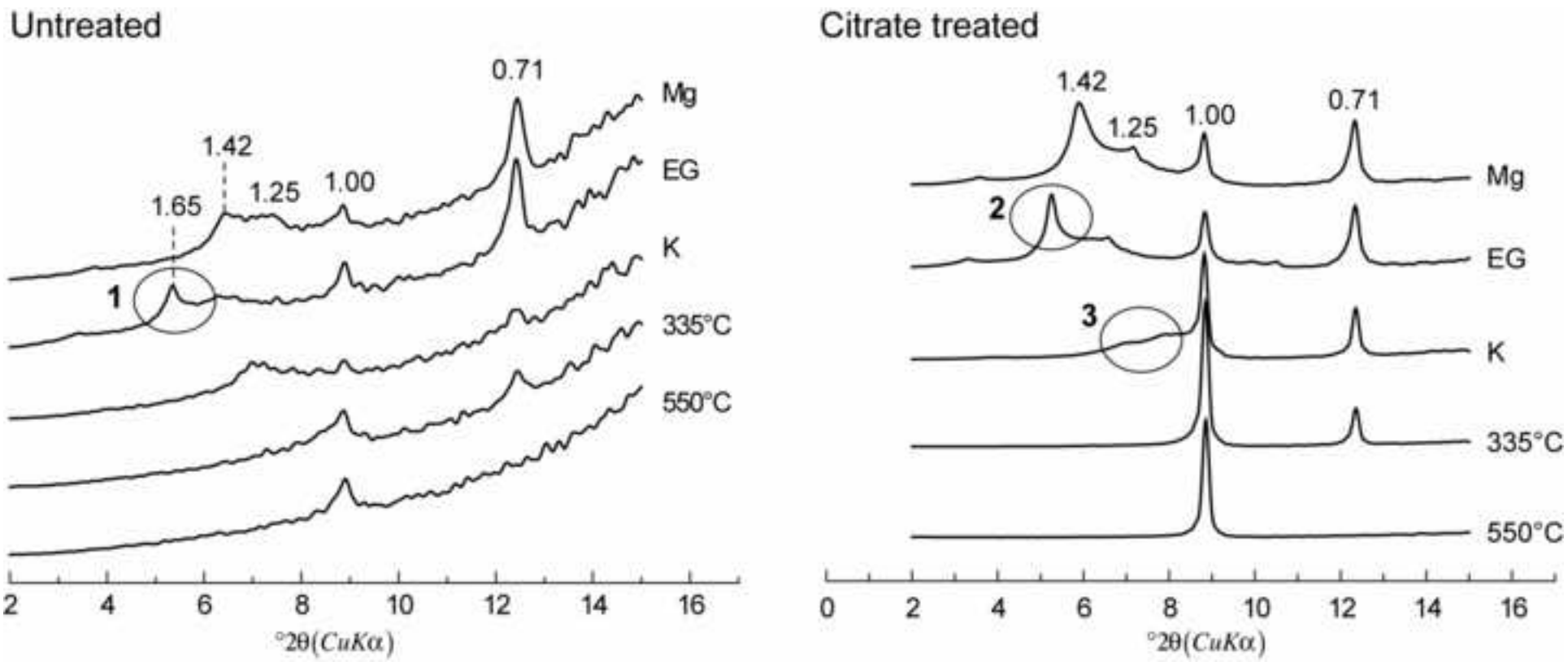

Figure 8

Click here to download high resolution image

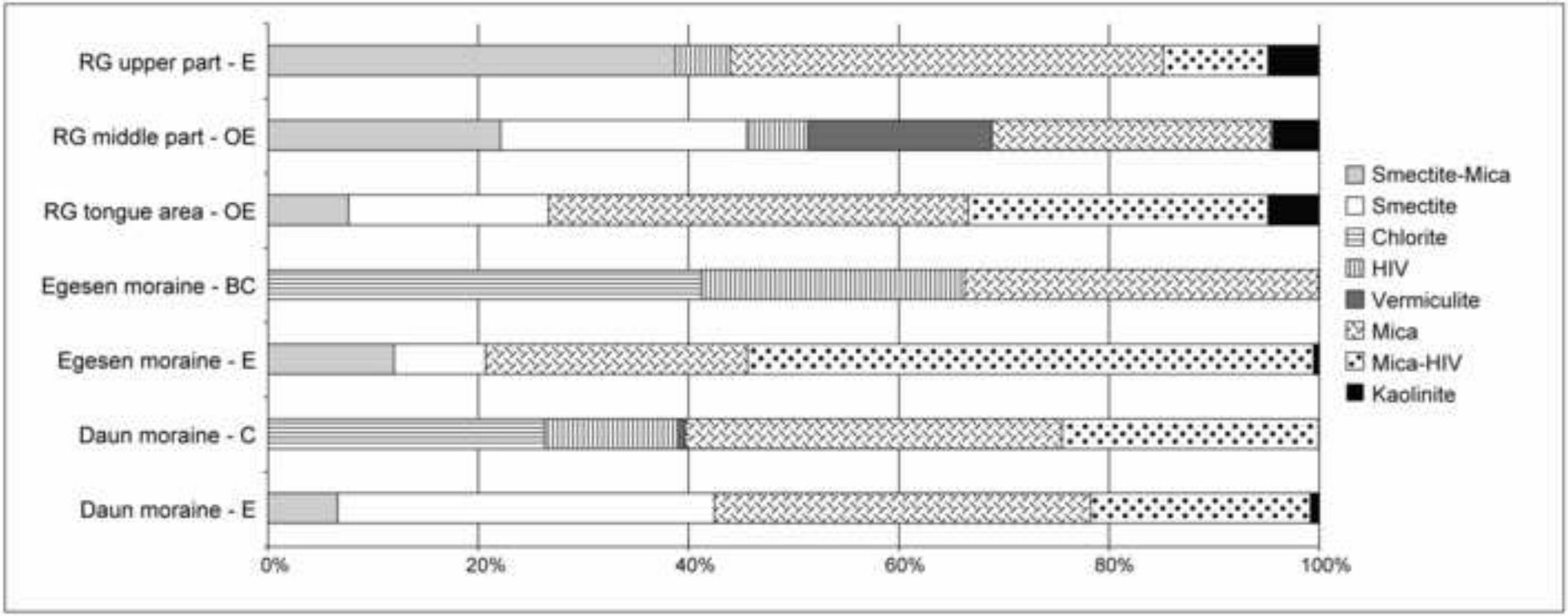

Figure 9

Click here to download high resolution image